Cell. Mol. Biol. (ISSN: 1165-158X)

Journal Homepage: www.cellmolbiol.org

Cellular and Molecular Biology

Original Article

Andrographolide influences IDD cell autophagy and oxidative stress under mechanical pressure via miR-9/FoxO3/PINK1/Parkin molecular axis

Jianwei Liu*, Dixing Lin, Jiadong Lu

Department of Spine Surgery, The Second Nanning People's Hospital,The Third Affiliated Hospital of Guangxi Medical University, Nanning, Guangxi, 530031, China

Article Info

Article history:

Received: January 16, 2024
Accepted: April 12, 2024
Published: June 30, 2024

Use your device to scan and read the article online

Abstract

Intervertebral disc degeneration (IDD) is characterized by the decreased function and number of nucleus pulposus cells (NPCs) caused by excessive intervertebral disc (IVD) pressure. This research aims to provide novel insights into IDD prevention and treatment by clarifying the effect of andrographolide (ANDR) on IDD cell autophagy and oxidative stress under mechanical stress. Human primary NPCs were extracted from the nucleus pulposus tissue of non-IDD trauma patients. An IDD cell model was established by posing mechanical traction on NPCs. Through the construction of an IDD rat model, the influence of ANDR on IDD pathological changes was explored *in vivo*. The proliferation and autophagy of NPCs were decreased while the apoptosis rate and oxidative stress reaction were increased by mechanical traction. ANDR intervention obviously alleviated this situation. MiR-9 showed upregulated expression in IDD cell model, while FoxO3 and PINK1/Parkin were downregulated. Decreased proliferation and autophagy as well as enhanced apoptosis and oxidative stress response of NPCs were observed following miR-9 mimics and H89 intervention, while the opposite trend was observed after FoxO3 overexpression. FoxO3 is a direct target downstream miR-9. The *in vivo* experiments revealed that after ANDR intervention, the number of apoptotic cells in rat IVD tissue decreased and the autophagy increased. In conclusion, ANDR improves NPC proliferation, and autophagy, inhibits apoptosis and oxidative stress, and alleviates the pathological changes of IDD via the miR-9/FoxO3/PINK1/Parkin axis, which may be a new and effective treatment for IDD in the future.

Keywords: Andrographolide; IDD; miR-9; FoxO3; PINK1/Parkin signaling pathway; Autophagy; Oxidative stress

1. Introduction

Intervertebral disc degeneration (IDD), an extremely common pathological process among the middle-aged and elderly, affects over 3 million patients worldwide [1]. IDD is the major cause of lower back pain in middle-aged and elderly people, which seriously affects people's daily lives and work [2]. At present, the clinical treatment of IDD is mainly based on physiotherapy and anti-inflammatory drugs; while for those with severe illness or ineffective conservative treatment, surgery is required to remove the nucleus pulposus [3]. IDD is a chronic process in which multiple factors are involved in the progressive destruction of the composition, structure and function of the intervertebral disc (IVD). In this process, the decline of the function and quantity of nucleus pulposus cells (NPCs) caused by excessive pressure of IVD is the pathological basis [4]. Substances such as Collagen II, proteoglycan and matrix metalloproteinase (MPP) secreted by NPCs are the key factors in maintaining the normal physiological function of IVD, so the functional impairment of NPCs can directly cause IVD connection reaction [5, 6]. Therefore, alleviating the functional damage of NPCs may be a new idea to relieve the pathological development of IDD.

Andrographolide (ANDR), a lactone diterpenoid isolated from Herba Andrographitis, has the pharmacological effects of heat-clearing and detoxicating, anti-inflammatory, anti-cancer and anti-oxidative stress [7]. It has been shown to exert a stable improvement effect on the functional decline of NPCs [8]. However, its specific mechanism remains poorly defined, and its relationship with IDD has yet to be confirmed. Forkhead box O3 (FoxO3) transcription factor, an important member of the FoxO subfamily, participates in the regulation of multiple biological processes such as apoptosis, cell cycle, immune response, and anti-oxidative stress [9]. Thompson et al. have confirmed that the expression of FoxO3 in NPCs isolated from the IDD mouse model decreased, but increased after treatment with theanine, an antioxidant drug [10]. Furthermore, FoxO3 can activate the PTEN-induced kinase 1 (PINK1)/Parkin pathway, promote mitochondrial autophagy and play a vital role in anti-oxidative stress [11], which also suggests that FoxO3 is a critical factor in regulating mitochondrial autophagy. FoxO3 transcriptional expression is affected by upstream targeted microRNAs, among which

* Corresponding author.
E-mail address: liujianwei@stu.gxmu.edu.cn (J.Liu).
Doi: http://dx.doi.org/10.14715/cmb/2024.70.6.29

microRNA-9 (miR-9) is an important regulator of organ development and neurogenesis, with a close association with cellular oxidative stress responses [12]. In the research of Zhang et al., it was found that miR-9 inhibited FoxO3 in cervical cancer cells [13]. All the preceding studies indicate the potential regulatory role of miR-9 and FoxO3 in IDD.

At present, it is of great significance to explore the role and mechanism of ANDR in regulating NPCs apoptosis under mechanical pressure for studying the pharmacological action of ANDR and the prevention and treatment of IDD. Based on the above studies, we speculate that its action pathway may be related to the miR-9/FoxO3/PINK1/Parkin signal transduction pathway, and therefore we conduct this research to experimentally confirm our view, providing effective reference for future clinical treatment of IDD.

2. Materials and methods

2.1. Cell data

Human primary NPCs were isolated from the nucleus pulposus of non-IDD trauma patients admitted to The Second Nanning People's Hospital, The Third Affiliated Hospital of Guangxi Medical University. The experimental protocols were approved by the Human Ethics Committee of The Second Nanning People's Hospital (approval No. Y2020061). After obtaining patients' informed consent, the nucleus pulposus tissue of non-IDD trauma patients was washed three times with PBS containing 1% penicillin and streptomycin under sterile conditions. The tissue was then cut into pieces and digested with 0.25% trypsin at 37℃ for 20 min. After 5 min of centrifugation (157×g, 4℃) to remove the supernatant, 0.1% type II collagenase was added for 4h of digestion at 37℃. Then, a 200-mesh sterile nylon mesh was used for filtration, and the supernatant was discarded after another 5 min of centrifugation (157×g, 4℃). After rinsing with DMEM/F12 medium three times, the samples were counted and inoculated in culture flasks, and cultured at 37℃ with 5%CO_2 in air.

2.2. IDD cell model establishment

Referring to the research of Kroeber[14], an IDD injury cell model was established based on the principle of direct mechanical traction with plexiglass and specially processed silicone elastic membrane as the main materials. The cells were seeded on the silica gel elastic membrane, which was stretched when the cell adherence reached 70-80%, so as to elongate the attached cells along with the unidirectional elongation of the elastic membrane. The elastic silica gel membrane was stretched by 40% via unidirectional stretching, and the negative pressure traction model was established after 12h of stretching. The membrane was digested and cultured in a Petri dish for later use.

2.3. ANDR intervention

The traction-cultured NPCs were inoculated on six-well plates, into which ANDR was added at the concentrations of 3 μg/mL, 6 μg/mL, and 9 μg/mL as low- (L-ANDR), medium- (M-ANDR) and high-concentration group (H-ANDR), respectively. In addition, NPCs with negative pressure traction but no ANDR intervention were set as the model group, and normal NPCs without negative pressure traction were set as the control group.

2.4. miR-9 intervention

IDD model cells were inoculated into 24-well plates at 1×10^5/well and were cultured in 500 μL serum-free medium when the cell density reached 70-80%. Then, miR-9 mimics sequence (miR-9-mimics) and negative control (miR-9-NC) were transfected into cells following the instructions of Lipofectamine 2000 (Thermo Fisher, USA). The transfection success rate was verified by PCR.

2.5. FoxO3 intervention

NPCs after negative pressure traction were transfected with FoxO3 overexpression vector and set as the FoxO3-si group. In addition, NPCs transfected with FoxO3 empty vector were included in the FoxO3-NC group, and the operation was the same as above.

2.6. PINK1/Parkin signaling pathway intervention

After negative pressure traction, NPCs were transfected with H89, a PINK1 upstream factor PKA inhibitor, and set as the H89 group. Another group of NPCs intervened by an equal amount of normal saline was set as the blank group.

2.7. CCK-8 assay

After trypsin digestion, NPCs in each intervention group were counted and inoculated into 96-well plates (100 μL/well). At 24 h, 48 h and 72 h of incubation, 10 μL of CCK8 (Abcam, China) were added into the wells for 2h of incubation. Then, the absorbance (optical density value; 450 nm) was determined using a microplate reader (BK-SY96A+ microplate reader, Shandong Boke Instrument Co., Ltd.) for cell viability analysis.

2.8. Flow cytometry (FCM)

Cells were digested with 0.25% trypsin and washed twice with pre-cooled PBS. Then NPCs of each group were fluorescently labeled with Annexin V-FITC (Sigma Aldrich, USA). After incubation at room temperature and PBS rinsing, the apoptosis rate of NPCs was measured by FCM (DxFLEX flow cytometer, Beckman Coulter, USA).

2.9. ELISA

The NPCs collected from each group were lysed and centrifuged (15200×g, 4℃) for 10 min to obtain the supernatant. Then, the contents of superoxide dismutase (SOD), malondialdehyde (MDA), glutathione peroxidase (GSH-Px) and reactive oxygen species (ROS) were detected according to the kit instructions, so as to assess the degree of oxidative stress response in cells. The kits were all purchased from Beijing Solarbio Science & Technology Co., Ltd.

2.10. QRT-PCR

The cells were inoculated in 6-well plates, and TRIzol was used to extract total RNA when the cell growth reached 80%. After the purity was verified, the cells were transcribed into cDNA according to the kit instructions (Thermo Fisher, USA), followed by the addition of SYBR green dye (Thermo Fisher) for PCR amplification. Reaction conditions: 2℃ for 2 min, 95℃ for 10 min, 96℃ for 15s, and 60℃ for 1 min, for a total of 40 cycles. With U6 as internal reference, the relative expression of target genes was calculated using the $2^{-\Delta\Delta Ct}$ method. Primer sequences were constructed by Nanjing GenScript

Biotechnology Co., Ltd. For miR-9, forward primer is CGGAGATCTTTTCTCTCTT, reverse primer is CAAGAATTCGCCCGAACCAG. For U6, forward primer is CTCGCTTCGGCAGCACA, reverse primer is AACGCTTCACGAATTTGCGT.

2.11. Western Blotting (WB)

The supernatant of RIPA-lysed cells was collected and denatured at 100℃ for 5 min. BCA (Abcam, China) was used to determine the protein concentration. Then, the protein membrane was electrophoresed by SDS-PAGE and transferred to a PVDF membrane, which was then sealed with 5% skim milk at room temperature for 1 h and incubated with primary antibodies overnight (4℃). The membrane was rinsed with TBST the next day and added with the secondary antibody. After ECL (Beyotime Biotechnology, China) development, the gray value of the PVDF membrane was analyzed.

2.12. Dual-luciferase reporter (DLR) assay

Starbase and Targetscan were used to predict the target genes of miR-9 and plot the Venn diagram. The fluorescence vectors containing FoxO3 3'UTR wild-type (FoxO3-WT) and mutant-type (FoxO3-MUT) were constructed and co-transfected with miR-9-mimics or miR-9-NC. The luciferase activity was determined 48h later using the DLR gene assay system (MedChemExpress, USA).

2.13. Rescue experiment

ANDR (9 μg/mL), miR-9-mimics, FoxO3-si and H89 were used simultaneously to intervene NPCs after negative pressure traction, which was set as Group A; NPCs simultaneously treated by ANDR (9 μg/mL), FoxO3-si and H89 after negative pressure traction were included in Group B; NPCs co-treated with ANDR (9 μg/mL) and H89 after negative pressure traction were assigned to Group C; NPCs intervened by ANDR (9 μg/mL) alone after negative pressure traction were set as group D; NPCs after negative pressure traction without any treatment were set as Group E. Cell proliferation, apoptosis, oxidative stress and autophagy were detected according to the above experiments.

2.14. Animal data

Fifteen 4-month-old male SPF SD rats, purchased from Zhongchong Bio-pharmaceutical (Taizhou) Co., Ltd. (Experimental animal license No.: SYXK (Su) 2021-0029), were water-deprivation one day before operation and weighed for anesthetic dose calculation. Pentobarbital sodium of 2% volume fraction was injected into the abdominal cavity of rats at 50 mg/kg for general anesthesia[15]. The animal experimental protocols were approved by the Animal Ethics Committee of The Second Nanning People's Hospital (approval No.202110082).

2.15. Establishment of an IDD animal model

Ten rats were randomly selected to establish a pressure-induced IDD rat model by referring a previous study [16]. After anesthesia, the rats were shaved from the abdomen for skin preparation (6 cm × 4 cm) when the pain reaction disappeared. The rats were positioned supine and sterilized with ethanol. A right para-median incision was made, and the skin and subcutaneous tissue were cut successively. Then, the abdominal cavity was opened, and the posterior peritoneum was cut to expose the L5 lumbar vertebrae and nerve roots. After the implantation of miniature silica gel balls, the subcutaneous fascia and skin of rats were sutured successively. The other 5 rats received no treatment and were set as the normal group.

2.16. ANDR therapy

ANDR was dissolved in 0.5% methylcellulose solution by referring to the previous research methods, and five IDD rats were randomly selected for fasting administration (150 mg/kg) as the intervention group. Another 5 rats in the IDD group were given the same amount of normal saline. Rats in each group were sacrificed after 3 weeks of continuous administration (once daily), and IVD tissues were collected for various tests.

2.17. TUNEL staining

Tissue paraffin sections of IVDs were dewaxed and hydrated with gradient ethanol, washed with PBS, and added with proteinase K (Sigma Aldrich). They were then incubated at room temperature for 15 min and immersed in sealing solution for 10 min. After PBS washing, the specimens were dripped with 50 μL TUNEL reaction solution (Sigma Aldrich) and then covered with glass slides for 1h in a dark room. Then, 50 μL of transforming agent was added dropwise for 30 min, followed by PBS washing and dropwise addition of DAB substrate for 10 min. Thereafter, the cells were re-dyed with hematoxylin, dehydrated with gradient alcohol after differentiation with HCL (Sigma Aldrich), transparentized with xylene, and mounted with neutral gum. Cell apoptosis was observed and photographed.

2.18. Immunofluorescence assay

After 20 min of fixation with paraformaldehyde (4%), the IVD tissue was washed with PBS, permeabilized with 0.1% Triton X-100 (Sigma Aldrich) for 10 min and blocked with 10% horse serum for 1h. This was followed by the addition of LC3 II primary antibody for overnight incubation (4℃). After 20 min of rewarming at room temperature as well as TBS washing, the tissue samples were incubated with a secondary antibody for 1h at ambient temperature. DAPI was added to dye the nuclei and the cells were incubated for 10 min in the dark. Finally, anti-fluorescence quencher was dripped for mounting, and the fluorescence intensity was observed under laser confocal microscopy.

2.19. Image analysis and pathological analysis

X-rays were performed on each group of rats at 7, 14, and 28 days after puncture of the model. The intervertebral disc height and upper and lower vertebral body heights were measured by blind method, and the intervertebral disc height index (DHI%) was calculated. The rat IDD model established in this study was evaluated by the Masuda intervertebral disc histopathology scoring method [17].

2.20. Statistical analysis

The software applied for statistical analysis was SPSS22.0. All the experiments in this study were repeatedly determined three times and the results were expressed by ($\bar{\chi}\pm s$). The inter-group comparison was performed by independent samples t test, and the multi-group comparison was conducted using one-way ANOVA and Bonfer-

roni post-hoc testing, with P values <0.05 indicating statistically significant differences.

3. Results

3.1. Effects of ANDR on cells

NPCs were infected with ANDR at doses of 3 μg/mL, 6 μg/mL, and 9 μg/mL, representing low- (L-ANDR), medium- (M-ANDR), and high-concentration groups (H-ANDR) respectively. First, through CCK-8 and FCM experiments, we found that the cell proliferation ability was significantly lower (Figure 1A), and the apoptosis rate (Figure 1B-C) was statistically higher in the model group compared with the control group. However, compared with the model group, CCK-8 indicated that the cell proliferation ability of the ANDR-intervened groups increased to some extent. While FCM analysis showed that the apoptosis rate decreased in ANDR-intervened groups. Among them, the H-ANDR group had the highest proliferation ability and the lowest apoptosis rate. Additionally, we analyzed the superoxide dismutase (SOD), malondialdehyde (MDA), glutathione peroxidase (GSH-Px) and reactive oxygen species (ROS) concentrations in different groups. ELISA showed that SOD and GSH-Px concentrations were the lowest and MDA and ROS concentrations were the highest in the model group compared to the control group. In ANDR-treated cells, SOD and GSH-Px were increased, with the highest levels observed in the H-ANDR group; the levels of MDA and ROS decreased and were the lowest in H-ANDR treated cells (Figure 1D). Subsequently, PCR (Figure 1E) and WB (Figure 1F-G) results identified that miR-9 expression was higher while FoxO3, PINK1/Parkin pathway protein and LC3-II protein levels were lower in the model group compared with the control group. Compared with the model group, miR-9 expression in the three ANDR-treated groups decreased, while FoxO3, PINK1/Parkin pathway protein and LC3-II protein levels increased, among which the changes were the most significant in the H-ANDR group.

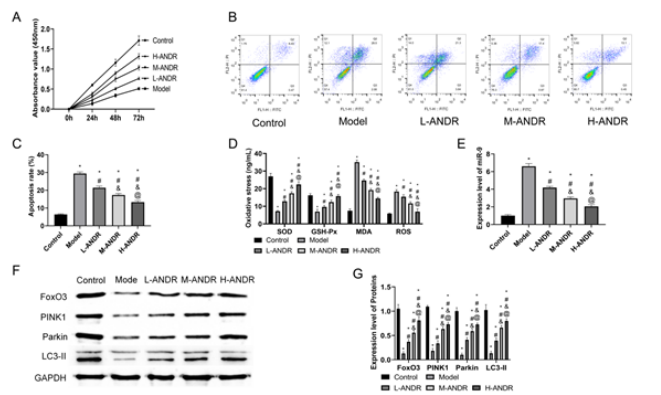

Fig. 1. Impacts of ANDR on cells. A) CCK-8 tested cell proliferation ability in control, model, and L/M/H-ANDR groups. B-C) Flow cytometry was used to evaluate NPCs apoptosis in control, model, L/M/H-ANDR groups, and the apoptosis rate of each group was statistically analyzed. D) ELISA assay was used to measure the concentration of SOD and MDA in different groups. E) Impacts of ANDR on miR-9 level in different NPCs groups by PCR. F-G) Impacts of ANDR on FoxO3, PINK1/Parkin pathway and autophagy protein in different NPCs groups by Western blotting, and the grayscale analysis of the expression of each protein was performed. Compared with the control group $^{*}P<0.05$. Compared with the model group $^{\#}P<0.05$. Compared with the L-ANDR group $^{\&}P<0.05$. Compared with the M-ANDR group $^{@}P<0.05$.

3.2. Effects of miR-9, FoxO3, and PINK1/Parkin pathway on cells

In order to explore the effect of miR-9 and FoxO3 in NPCs, NPCs were transfected with miR-9-mimics and si-FoxO3 after negative pressure traction. After successful transfection of miR-9-mimics (Figure 2A), cell proliferation ability (Figure 2B) was significantly lower while the apoptosis (Figure 2C) was higher in the miR-9-mimics group compared with the miR-9-NC group. ELISA showed that the contents of SOD and GSH-Px in the miR-9-mimics group decreased, while MDA and ROS increased (Figure 2D). Furthermore, WB determined lower FoxO3, PINK1/Parkin pathway protein and LC3-II protein levels in the miR-9-mimics group compared with the miR-9-NC group (Figure 2E-F).

On the contrary, After successful transfection of FoxO3-si (Figure 3A), silencing of FoxO3 by FoxO3-si increased cell proliferation ability (Figure 3B), decreased apoptosis rate (Figure 3C), caused higher SOD and GSH-Px contents and lower MDA and ROS contents (Figure 3D), and enhanced PINK1/Parkin pathway protein and LC3-II protein levels (Figure 3E-F).

Next, to effects of PINK1/Parkin pathway on NPCs were assessed we transfected H89, a PINK1 upstream factor PKA inhibitor, in NPCs after negative pressure traction. The H89 group exhibited lower cell proliferation capacity (Supplementary Figure 1A) and higher apoptosis (Supplementary Figure 1B-C) than the blank group. The results of ELISA showed lower SOD and GSH-Px contents and higher MDA and ROS contents in the H89 group compared with the blank group (Supplementary Figure 1D). The autophagy protein detection test showed that the expression of LC3-II in the H89 group was lower than that in the blank group (Supplementary Figure 1E-F).

3.3. ANDR influences IDD cell effects via miR-9/FoxO3/PINK1/Parkin molecular axis

First, through online target gene prediction websites

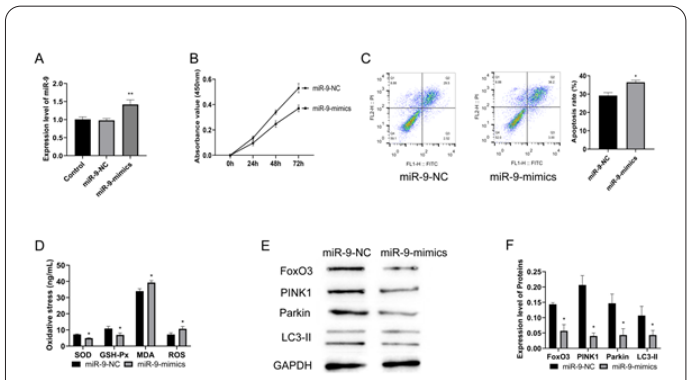

Fig. 2. Impacts of miR-9 on cells. A) The expression of miR-9 was detected by PCR after transfection of miR-9-NC and miR-9-mimics. B) CCK-8 was used to test cell proliferation ability in miR-9-NC and miR-9-mimics groups. C) Flow cytometry was used to detect cell apoptosis in miR-9-NC and miR-9-mimics groups. D) ELISA assay was used to measure the concentration of SOD, GSH-Px, ROS and MDA in miR-9-NC and miR-9-mimics groups. E-F) Impacts of miR-9 on FoxO3, PINK1/Parkin pathway and autophagy protein in NPCs by Western blotting. Compared with the miR-9-NC group $^{*}P<0.05$.

Starbase and Targetscan (Figure 4A). TargetScan demonstrated that FoxO3 was a potential downstream mRNA of miR-9 possessing binding sequence at FoxO3 3'UTR (Figure 4B). Subsequently, Dual-luciferase reporter assay showed that the fluorescence activity of FoxO3-WT was obviously inhibited after miR-9-mimics transfection (Figure 4C), which indicated that there was a targeted regulation relationship between FoxO3 and miR-9. Besides, PCR findings indicated that the expression of FoxO3 was decreased after miR-9 overexpression (Figure 4D). Finally, in the rescue experiment, we found no difference in cell proliferation ability (Figure 4E) and apoptosis rate (Figure 4F-G) among groups A, C, and E, and no difference between groups B and D (P>0.05); Among them, the proliferation ability was lower, and the apoptosis rate was higher in groups A, C, and E compared with groups B and D. WB results also showed no significant difference in LC3-II protein expression among groups A, C, and E, lower than that in groups B and D (Figure 4H).

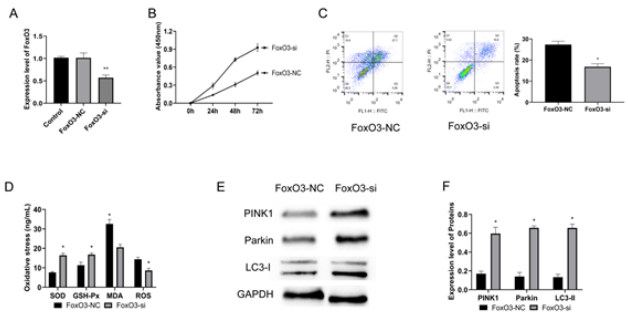

Fig. 3. Impacts of FoxO3 on cells. A) The expression of FoxO3 was detected by PCR after transfection of FoxO3-NC and FoxO3-si. B) CCK-8 was used to detect cell proliferation ability in FoxO3-NC and FoxO3-si groups. C) Flow cytometry was used to detect cell apoptosis in FoxO3-NC and FoxO3-si groups. D) ELISA assay was used to measure the concentration of SOD, GSH-Px, ROS and MDA in FoxO3-NC and FoxO3-si groups. E-F) Impacts of FoxO3 on PINK1/Parkin pathway and autophagy protein in NPCs by Western blotting. Compared with the FoxO3-NC group *P<0.05.

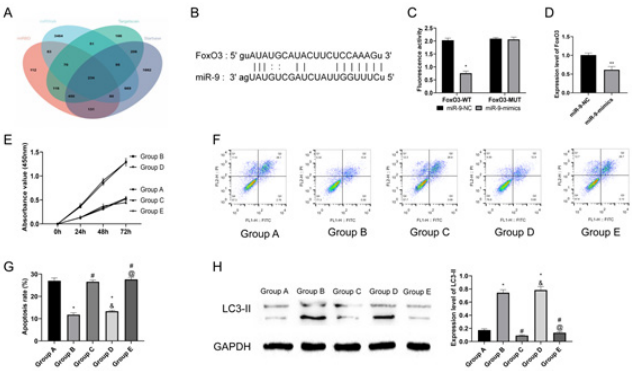

Fig. 4. ANDR influences IDD cell effects via miR-9/FoxO3/PINK1/Parkin molecular axis. A) The relationship between miR-9 and FoxO3 analyzed by online target gene prediction websites Starbase and Targetscan. B) The complementary sites where miR-9 and FoxO3 can bind. C) Dual-luciferase reporter assay was used to detect the binding abundance of FoxO3 to miR-9. D) PCR tested the expression of FoxO3 after miR-9-mimics transfection. E) CCK-8 was used to detect cell proliferation ability in A-E groups. F-G) Flow cytometry was used to detect cell apoptosis in A-E groups. H) Western blotting tested the expression of LC3-II protein in A-E groups. Compared with Group A *P<0.05. Compared with Group B #P<0.05. Compared with Group C &P<0.05. Compared with Group D @P<0.05.

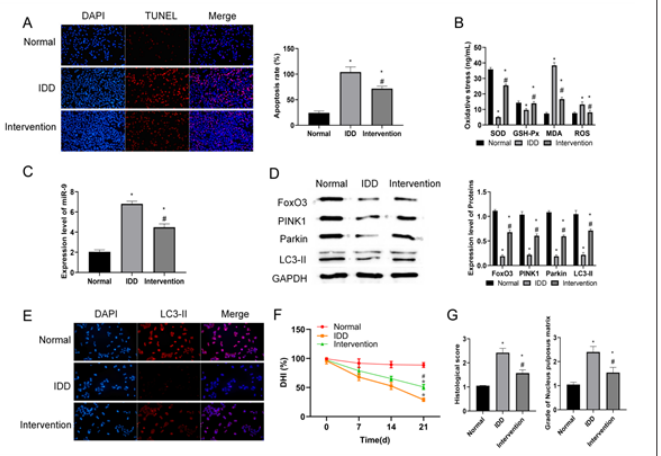

Fig. 5. In vivo experiment. A) The number of NPCs apoptosis in normal rats, pressure-induced IDD rat model, and intervention (fasting administration) rat intervertebral disc tissue by TUNEL staining. B) ELISA assay detected the impacts of ANDR on the levels of SOD, GSH-Px, MDA and ROS in IDD rats' intervertebral disc. C) The expression of miR-9 in normal, IDD, and intervention rat intervertebral disc tissue by PCR. D) The expression of FoxO3, PINK1, Parkin, and LC3-II in normal, IDD, and intervention rat intervertebral disc tissue by Western blotting. E) Fluorescence intensity of LC3-II protein in normal, IDD, and intervention rat intervertebral disc tissue. Compared with the normal group *P<0.05. Compared with the IDD group #P<0.05.

3.4. In vivo experiment

We establish a pressure-induced IDD rat model, and IDD rats were randomly selected for fasting administration (150 mg/kg) as the intervention group. First, TUNEL staining identified that the number of IVD cell apoptosis in the intervention group, higher than that in the normal group, was significantly lower than that in the IDD group (Figure 5A). The results of ELISA also showed that SOD and GSH-Px contents in rat IVD tissue in the intervention group were lower than those of the normal group but higher than the IDD group, while MDA and ROS contents were higher than those of the normal group but lower than the IDD group (Figure 5B). Furthermore, the results of PCR (Figure 5C) and WB (Figure 5D) revealed that LC3-II protein expression in the IVD tissue of the intervention group had no difference from that of the normal group (P>0.05), higher than that of the IDD group; miR-9 expression was higher than that of the normal group, but was significantly lower compared with the IDD group; FoxO3 and PINK1/Parkin pathway protein levels were lower than those in the normal group and higher than those in the IDD group. Moreover, the expression of autophagy proteins was verified by immunofluorescence experiment, and the results also showed that the fluorescence intensity of LC3-II protein in the intervention group was lower than that in the normal group, but higher than that in the IDD group (Figure 5E).

In addition, in normal rats, there was no significant difference in IVD height at L5 at various time points (Figure 5F), and all rat NPs were intact oval in shape with intact extracellular matrix (Figure 5G). In the IDD rats, the IVD

height was reduced (Figure 5F), the NP structure was incomplete, the subchondral bone was significantly damaged, and the extracellular matrix was basically missing (Figure 5G), suggesting obvious IDD. After the ANDR intervention, the height of degenerative IVD was elevated (Figure 5F), and the tissue morphology improved (Figure 5G), suggesting a significant improvement in IDD.

4. Discussion

In this study, we found that ANDR has a significant improvement effect on IDD model cells, and its mechanism may be related to the miR-9/FoxO3/PINK1/Parkin axis, which is of great significance for future treatment of IDD. Mechanical load-induced apoptosis of NPCs is an important cause of IDD, and oxidative stress is the pathogenesis [18]. In addition, autophagy is one of the representative reactions of IDD. Mitochondrial autophagy is an important pathway of cellular antioxidation, and the pathogenesis of IDD is precisely due to the reduction of autophagy ability, which leads to aggravation of intracellular oxidative and inflammatory responses, resulting in a large number of cell apoptosis and inflammatory lesions [19]. ANDR has been proven to exert pharmacological effects such as clearing heat and detoxication, anti-inflammatory, anticancer and anti-oxidation [20]. We established an IDD cell model through pressure traction of NPCs. Following ANDR intervention, we observed significantly ameliorated cell proliferation and oxidative stress response of IDD model cells and reduced apoptosis. In addition, the reversal of autophagic protein expression intervened by ANDR suggests whether ANDR can promote autophagy in IDD cells, which requires the use of autophagy inhibitors to verify autophagic flux. Therefore, ANDR may become a new treatment option for future clinical treatment of IDD.

We also found that the expression of miR-9 was upregulated in IDD model cells, while FoxO3 and PINK1/Parkin levels were decreased. However, under ANDR intervention, miR-9 in IDD model cells decreased, while FoxO3, PINK1/Parkin increased, suggesting that ANDR affected the molecular modification pathway, which may also be the mechanism underlying the effect of ANDR on IDD. Ectopic expression of miR-9 down-regulated the expression of ROS scavenging enzymes SOD, GSH-Px, CAT and GSH-Px, which led to increased ROS production, and inhibited expression of transcription factor FoxO3, thus blocking the signal pathway of erythropoiesis[21]. These results suggest that miR-9 participates in cell survival through the regulatory mechanism of cellular oxidative stress. We found that the increase of miR-9 expression can accelerate the damage of IDD cells. In a previous study, miR-9 was abnormally elevated in A549 cells and significantly inhibited the autophagy of A549 cells [22]. Similarly, our study shows that miR-9 can inhibit the PINK1/Parkin pathway and can inhibit the expression of the autophagic protein FoxO3.

When the body is under oxidative stress, the accumulated ROS makes FoxO3 undergo post-translational modifications such as phosphorylation/dephosphorylation and acetylation/acetylation, thus promoting the exacerbation of oxidative stress responses [23]. Furthermore, phosphorylation of FoxO3 can promote nuclear translocation, improve its transcription activity, and regulate downstream signal pathways to change the apoptosis ability of cells [24]. In this study, we verified the correlation between FoxO3 and IDD cell apoptosis capacity and emphasized the important role of FoxO3 in IDD. Next, we confirmed that the PINK1/Parkin pathway also had a significant impact on the IDD cell damage process. Furthermore, we found a targeted regulatory relationship between miR-9 and FoxO3, which further confirmed our view that ANDR affects IDD through the miR-9/FoxO3/PINK1/Parkin signal transduction pathway.

Subsequently, through the rescue experiment, we obtained the following results: (1) The influence of FoxO3-si on cells was reversed by H89; (2) Impacts of ANDR can be reversed by miR-9-mimics. (3) The regulation of cell damage by ANDR can be inversely modulated by miR-9/FoxO3/PINK1/Parkin, confirming their relationship. Finally, *in vivo* experiments determined that ANDR could influence the pathological damage of IDD through the miR-9/FoxO3/PINK1/Parkin molecular axis.

However, in addition to mechanical stress, severe peroxidation damage is also the key to accelerating the apoptosis of NPCs in the pathological development of IDD. Therefore, in the follow-up research, we need to further confirm the role of ANDR and miR-9/FoxO3/PINK1/Parkin through the IDD cell model under the peroxide state. In addition, the observation of the pathological changes of IDD mouse IVD under the intervention of ANDR is warranted. Finally, we will conduct human trials as soon as possible to confirm the clinical use of ANDR and provide reliable reference for the prevention and treatment of IDD in the future.

5. Conclusion

ANDR improves the proliferation and autophagy of IDD model cells via the miR-9/FoxO3/PINK1/Parkin molecular axis, inhibits cell apoptosis and oxidative stress, and alleviates the pathological changes of IDD, which may be a new effective treatment for IDD in the future.

Acknowledgements

This work was supported by the Guangxi Natural Science Foundation (NO: 2021GXNSFAA075007) and 139 Program of Guangxi Medical High-level Backbone Talents (NO: G202003021).

Declaration of Competing Interest

No potential conflict of interest was reported by the authors.

Availability of data and materials

The datasets used and/or analyzed during the current study are available from the corresponding author on reasonable request.

Authors contribution statement

Jianwei Liu designed the study, wrote, and revised the manuscript. Dixing Lin collected and analyzed data. Jiadong Lu organized and visualized data. All authors agreed to be accountable for all aspects of the work and approved the final submitted manuscript.

References

1. Battié MC, Joshi AB, Gibbons LE (2019) Degenerative Disc Disease: What is in a Name? Spine 44 (21): 1523-1529. doi: 10.1097/brs.0000000000003103

2. Kim HS, Wu PH, Jang IT (2020) Lumbar Degenerative Disease Part 1: Anatomy and Pathophysiology of Intervertebral Discogenic Pain and Radiofrequency Ablation of Basivertebral and Sinuvertebral Nerve Treatment for Chronic Discogenic Back Pain: A Prospective Case Series and Review of Literature. International journal of molecular sciences 21 (4). doi: 10.3390/ijms21041483
3. Fusellier M, Clouet J, Gauthier O, Tryfonidou M, Le Visage C, Guicheux J (2020) Degenerative lumbar disc disease: in vivo data support the rationale for the selection of appropriate animal models. European cells & materials 39: 18-47. doi: 10.22203/eCM.v039a02
4. Swanson BT, Creighton D (2020) The degenerative lumbar disc: not a disease, but still an important consideration for OMPT practice: a review of the history and science of discogenic instability. The Journal of manual & manipulative therapy 28 (4): 191-200. doi: 10.1080/10669817.2020.1758520
5. Reid PC, Morr S, Kaiser MG (2019) State of the union: a review of lumbar fusion indications and techniques for degenerative spine disease. Journal of neurosurgery Spine 31 (1): 1-14. doi: 10.3171/2019.4.Spine18915
6. Rogerson A, Aidlen J, Jenis LG (2019) Persistent radiculopathy after surgical treatment for lumbar disc herniation: causes and treatment options. International orthopaedics 43 (4): 969-973. doi: 10.1007/s00264-018-4246-7
7. Burgos RA, Alarcón P, Quiroga J, Manosalva C, Hancke J (2020) Andrographolide, an Anti-Inflammatory Multitarget Drug: All Roads Lead to Cellular Metabolism. Molecules (Basel, Switzerland) 26 (1). doi: 10.3390/molecules26010005
8. Xu L, Cai P, Li X, Wu X, Gao J, Liu W, Yang J, Xu Q, Guo W, Gu Y (2021) Inhibition of NLRP3 inflammasome activation in myeloid-derived suppressor cells by andrographolide sulfonate contributes to 5-FU sensitization in mice. Toxicology and applied pharmacology 428: 115672. doi: 10.1016/j.taap.2021.115672
9. Lee JW, Nam H, Kim LE, Jeon Y, Min H, Ha S, Lee Y, Kim SY, Lee SJ, Kim EK, Yu SW (2019) TLR4 (toll-like receptor 4) activation suppresses autophagy through inhibition of FOXO3 and impairs phagocytic capacity of microglia. Autophagy 15 (5): 753-770. doi: 10.1080/15548627.2018.1556946
10. Thompson MG, Larson M, Vidrine A, Barrios K, Navarro F, Meyers K, Simms P, Prajapati K, Chitsike L, Hellman LM, Baker BM, Watkins SK (2015) FOXO3-NF-κB RelA Protein Complexes Reduce Proinflammatory Cell Signaling and Function. Journal of immunology (Baltimore, Md : 1950) 195 (12): 5637-5647. doi: 10.4049/jimmunol.1501758
11. Hu J, Liu T, Fu F, Cui Z, Lai Q, Zhang Y, Yu B, Liu F, Kou J, Li F (2022) Omentin1 ameliorates myocardial ischemia-induced heart failure via SIRT3/FOXO3a-dependent mitochondrial dynamical homeostasis and mitophagy. Journal of translational medicine 20 (1): 447. doi: 10.1186/s12967-022-03642-x
12. Liu J, Zuo X, Han J, Dai Q, Xu H, Liu Y, Cui S (2020) MiR-9-5p inhibits mitochondrial damage and oxidative stress in AD cell models by targeting GSK-3β. Bioscience, biotechnology, and biochemistry 84 (11): 2273-2280. doi: 10.1080/09168451.2020.1797469
13. Zhang H, Zhang Z, Wang S, Zhang S, Bi J (2018) The mechanisms involved in miR-9 regulated apoptosis in cervical cancer by targeting FOXO3. Biomedicine & pharmacotherapy = Biomedecine & pharmacotherapie 102: 626-632. doi: 10.1016/j.biopha.2018.03.019
14. Kroeber M, Unglaub F, Guehring T, Nerlich A, Hadi T, Lotz J, Carstens C (2005) Effects of controlled dynamic disc distraction on degenerated intervertebral discs: an in vivo study on the rabbit lumbar spine model. Spine 30 (2): 181-187. doi: 10.1097/01.brs.0000150487.17562.b1
15. Mao S, Huang H, Chen X (2022) κlncRNA H19 Aggravates Brain Injury in Rats following Experimental Intracerebral Hemorrhage via NF-B Pathway. Computational and mathematical methods in medicine 2022: 3017312. doi: 10.1155/2022/3017312
16. Kim H, Hong JY, Lee J, Jeon WJ, Ha IH (2021) IL-1β promotes disc degeneration and inflammation through direct injection of intervertebral disc in a rat lumbar disc herniation model. The spine journal : official journal of the North American Spine Society 21 (6): 1031-1041. doi: 10.1016/j.spinee.2021.01.014
17. Masuda K, Aota Y, Muehleman C, Imai Y, Okuma M, Thonar EJ, Andersson GB, An HS (2005) A novel rabbit model of mild, reproducible disc degeneration by an anulus needle puncture: correlation between the degree of disc injury and radiological and histological appearances of disc degeneration. Spine 30 (1): 5-14. doi: 10.1097/01.brs.0000148152.04401.20
18. Abi-Hanna D, Kerferd J, Phan K, Rao P, Mobbs R (2018) Lumbar Disk Arthroplasty for Degenerative Disk Disease: Literature Review. World neurosurgery 109: 188-196. doi: 10.1016/j.wneu.2017.09.153
19. Xie L, Huang W, Fang Z, Ding F, Zou F, Ma X, Tao J, Guo J, Xia X, Wang H, Yu Z, Lu F, Jiang J (2019) CircERCC2 ameliorated intervertebral disc degeneration by regulating mitophagy and apoptosis through miR-182-5p/SIRT1 axis. Cell death & disease 10 (10): 751. doi: 10.1038/s41419-019-1978-2
20. Gao J, Peng S, Shan X, Deng G, Shen L, Sun J, Jiang C, Yang X, Chang Z, Sun X, Feng F, Kong L, Gu Y, Guo W, Xu Q, Sun Y (2019) Inhibition of AIM2 inflammasome-mediated pyroptosis by Andrographolide contributes to amelioration of radiation-induced lung inflammation and fibrosis. Cell death & disease 10 (12): 957. doi: 10.1038/s41419-019-2195-8
21. Wang Z, Sun L, Jia K, Wang H, Wang X (2019) miR-9-5p modulates the progression of Parkinson's disease by targeting SIRT1. Neuroscience letters 701: 226-233. doi: 10.1016/j.neulet.2019.02.038
22. Zhang Y, Meng X, Li C, Tan Z, Guo X, Zhang Z, Xi T (2017) MiR-9 enhances the sensitivity of A549 cells to cisplatin by inhibiting autophagy. Biotechnology letters 39 (7): 959-966. doi: 10.1007/s10529-017-2325-2
23. Hwang I, Uchida H, Dai Z, Li F, Sanchez T, Locasale JW, Cantley LC, Zheng H, Paik J (2021) Cellular stress signaling activates type-I IFN response through FOXO3-regulated lamin posttranslational modification. Nature communications 12 (1): 640. doi: 10.1038/s41467-020-20839-0
24. Deng A, Ma L, Zhou X, Wang X, Wang S, Chen X (2021) FoxO3 transcription factor promotes autophagy after oxidative stress injury in HT22 cells. Canadian journal of physiology and pharmacology 99 (6): 627-634. doi: 10.1139/cjpp-2020-0448